Model of the Conical-scanning Microwave Imager/Sounder (center) with a model of the DMSP Special Sensor Microwave/Imager (right) and a microwave imager for the Tropical Rainfall Measurement Mission (left). CMIS, a multiband radiometer that will be deployed on NPOESS, integrates many features of heritage conical-scanning radiometers into a single radiometer. It will offer several new operational products (sea surface wind direction, soil moisture, and cloud base height) and quantifiable resolution and measurement range improvements over existing remotely sensed environmental products.
Boeing Space Systems

Active Microwave Radar

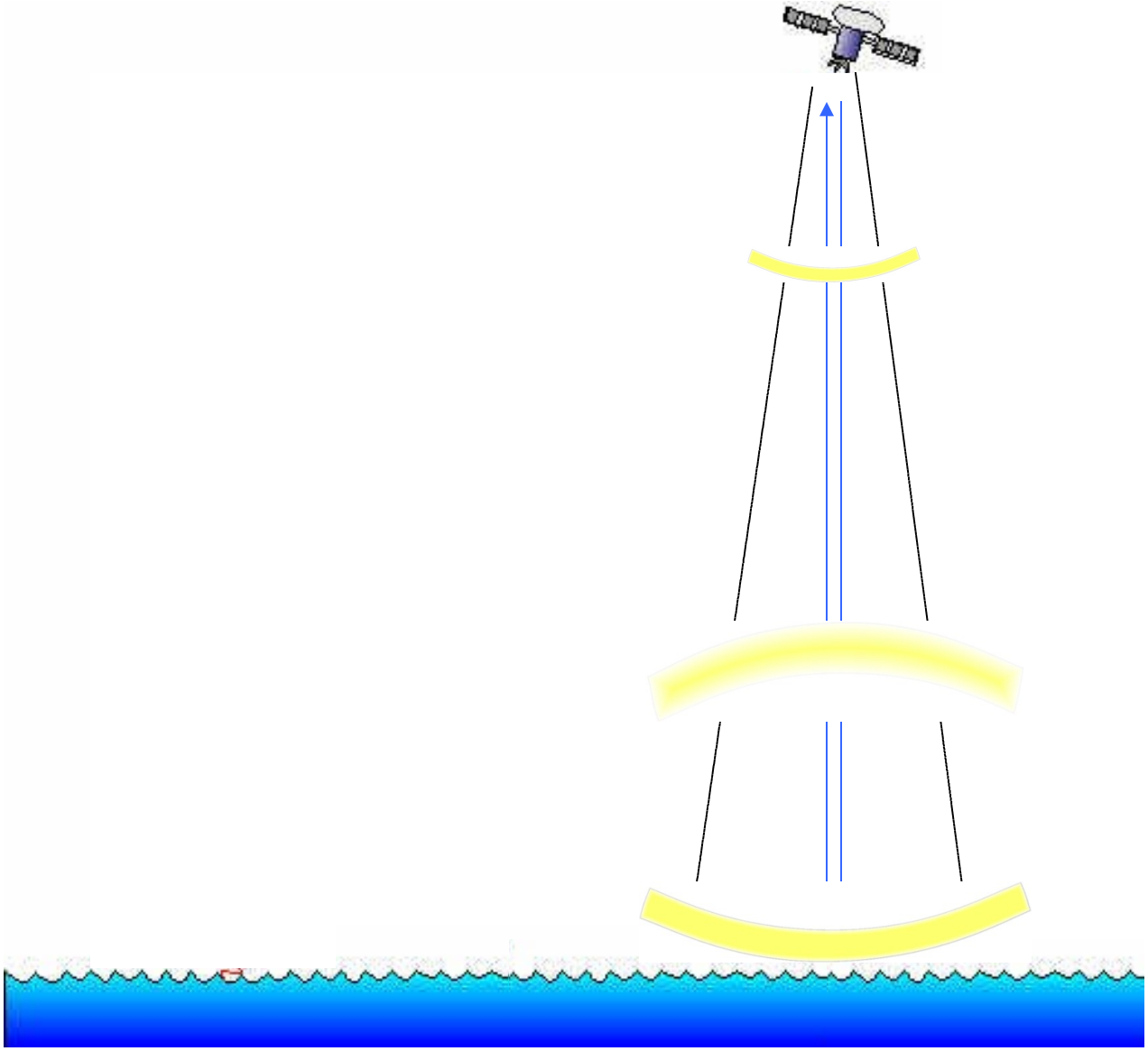

Reflection difference between rough and smooth surface

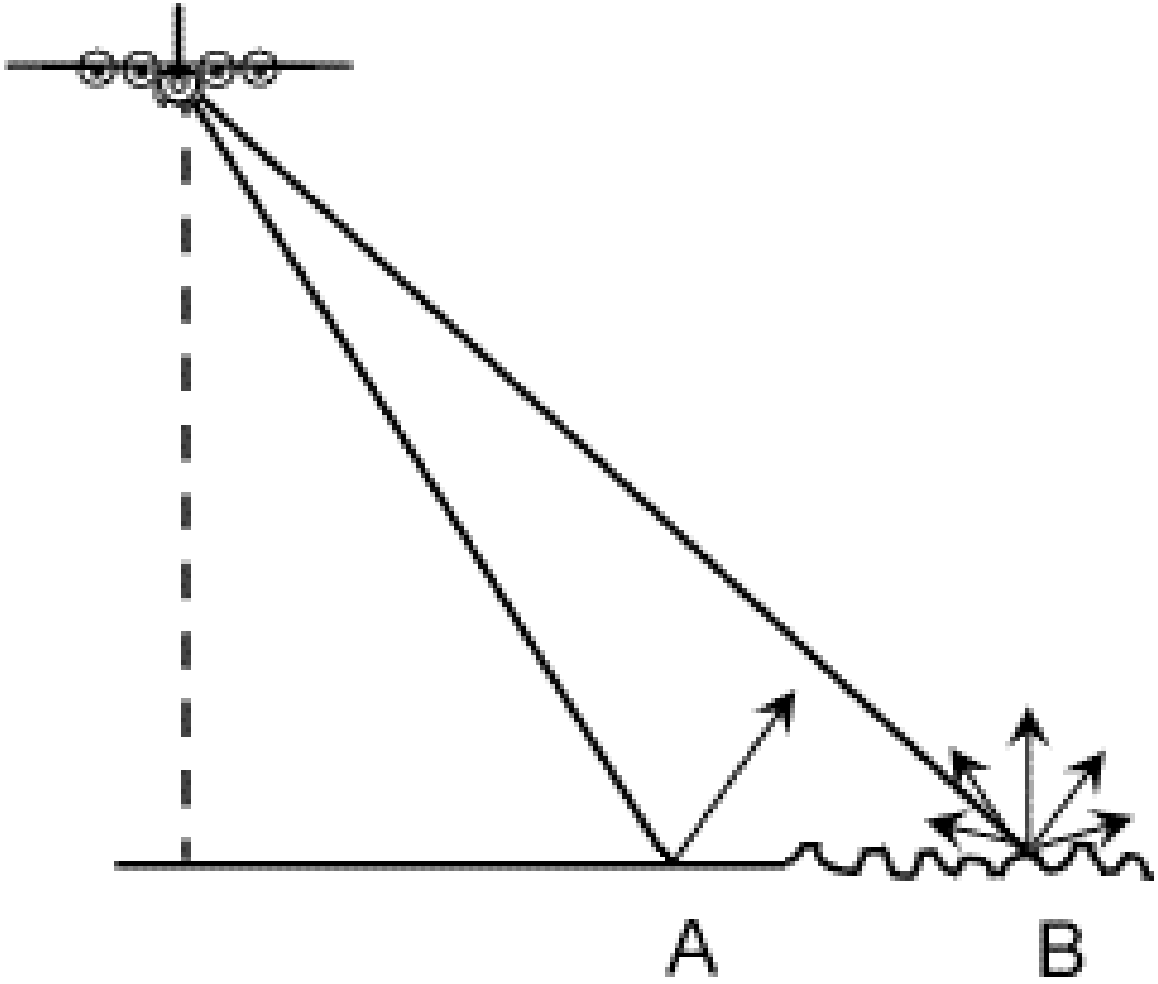

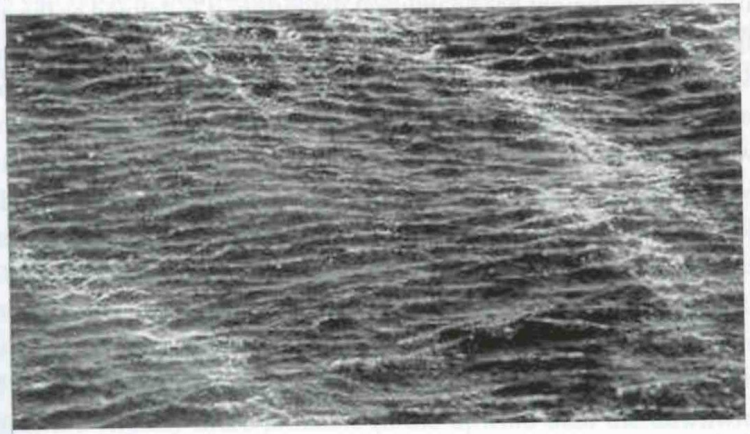

Scattering cross Section, σ_o

(1) Specular Reflection

Near vertical incidence

reflection off mirror-like facets

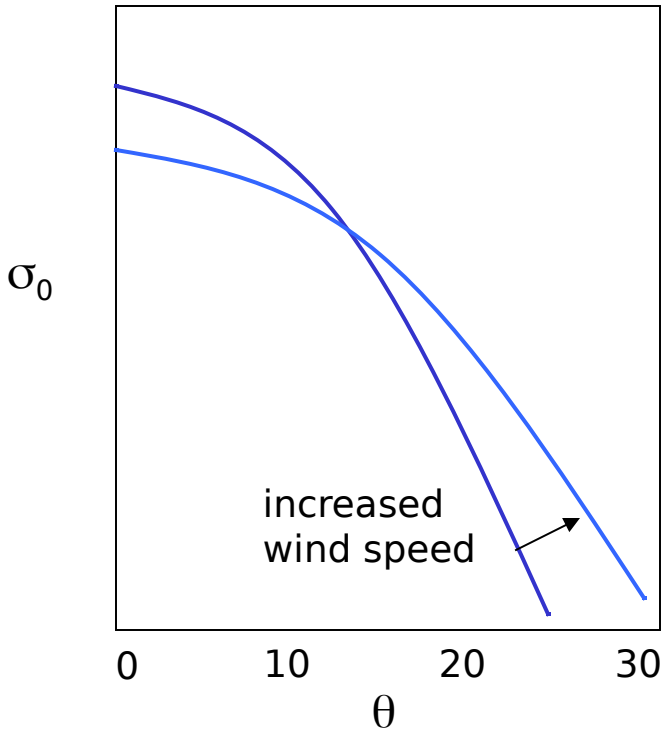

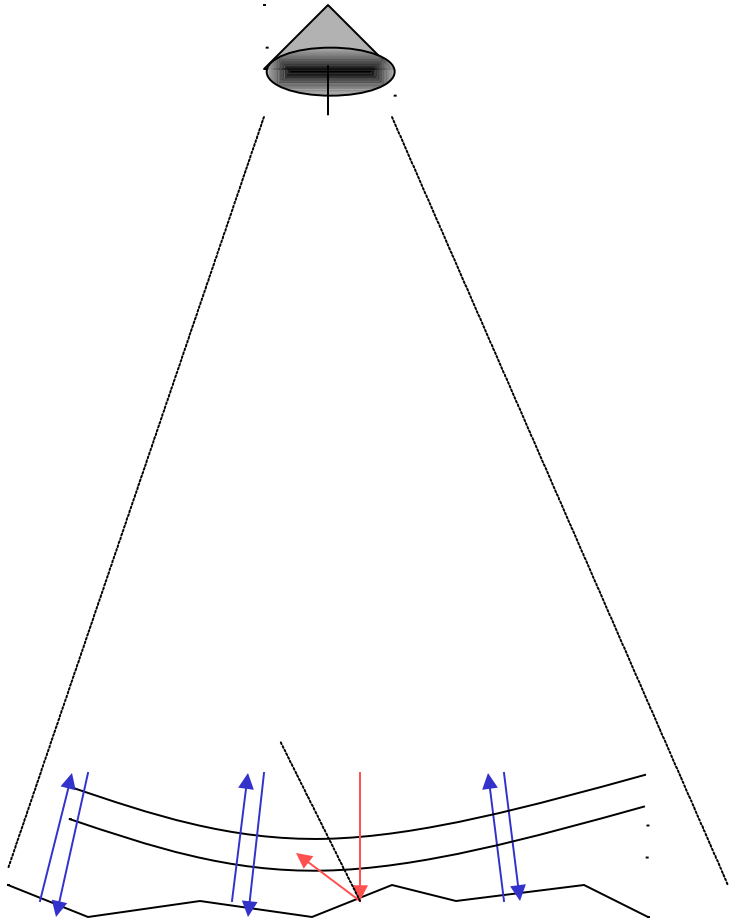

Important for θ < 20° (there are almost no wave slopes > 25°)

(2) Resonant (Bragg) Scatter

θ> 20° (occurs at all θ but dominates here)

off-nadir so polarization is important

Ocean wave-length of importanc $L_B = \frac{\lambda}{2\sin\theta}$

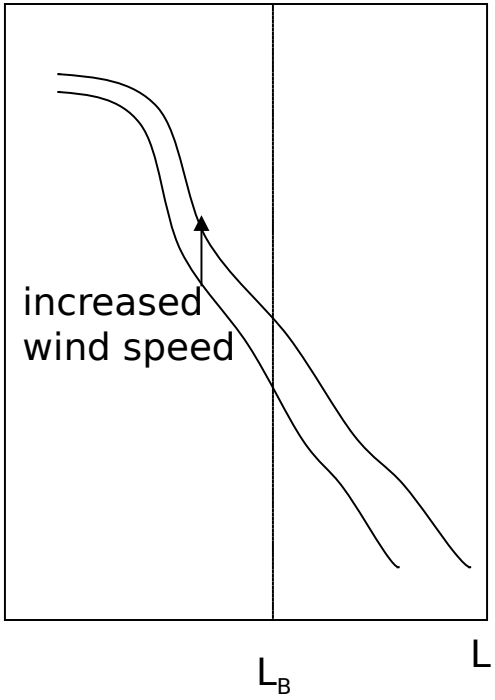

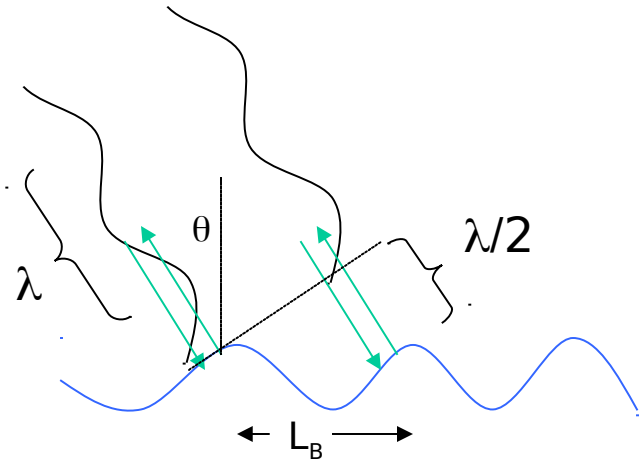

- Bragg Scatter Equation:

$$\lambda_s = \frac{n\lambda_r}{2\sin\theta}$$

- the wavelength of the surface roughness (λ_s) that will give the maximum radar return for radar wavelength (λ_r)

  - For Ku band: $\lambda_s \sim 3$ cm (Seasat)
  - For C band: $\lambda_s \sim 6$ cm (ERS-1/2)

Backscatter Mechanism

- Assumed to be dominated by Bragg Scattering at incidence angles $\theta > 25^{o}$ from vertical
- Backscatter due to in-phase reflections from surface
- Constructive interference

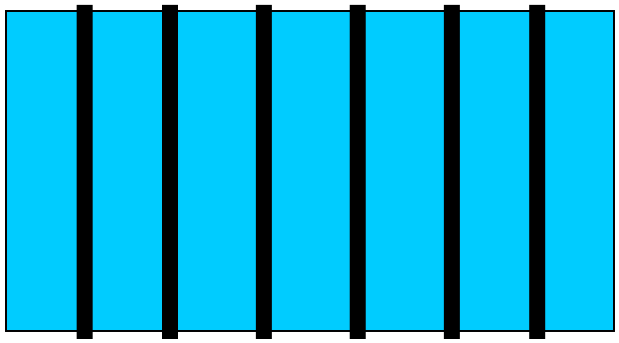

Constructive Interference

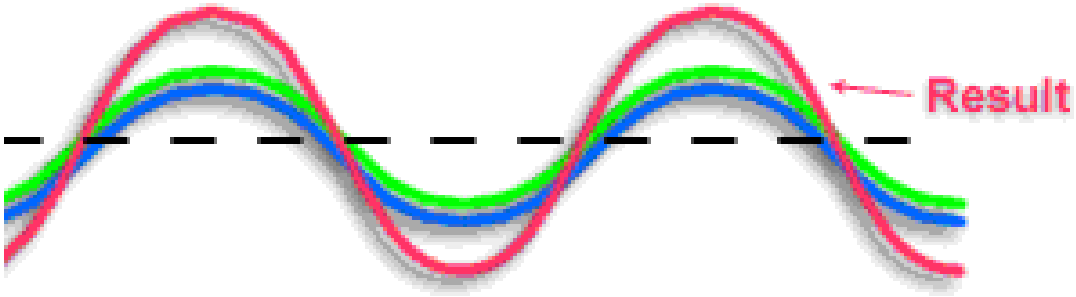

Destructive Interference

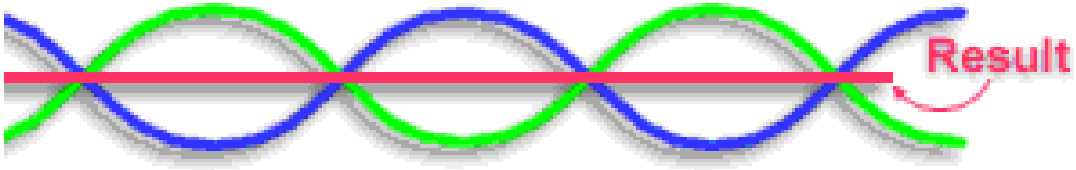

Example of Homogeneous Target
(being imaged by a radar sensor)

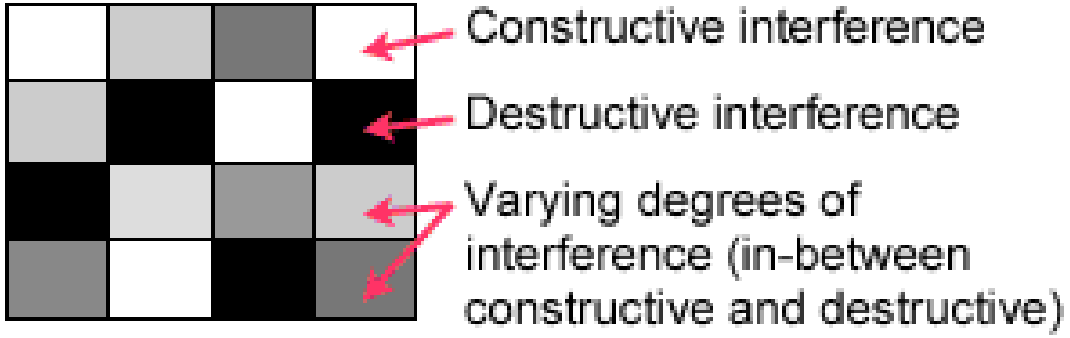

σ_o depends on:

- Polarization
- Wavelength
- zenith angle
- wave spectrum (are there enough L_B's?) and wave spectrum in 2-D projection of L_B fronts along line of sight

Factors Influencing Scattering

- Sea surface temperature
- Sea state
- Fetch
- Surface slicks (oil, biology)
- Rain
- Land

These factors can introduce large errors into scatterometer wind fields

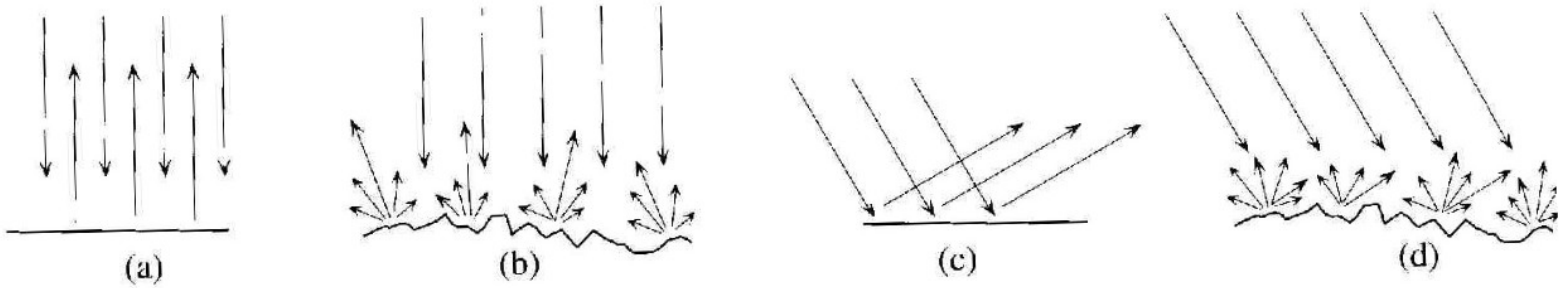

Figure 10.13. The specular reflection and incoherent scattering of a radiance incident on a surface. (a) Normal incidence, specular surface; (b) normal incidence, wave-covered surface; (c) oblique incidence, specular surface; (d) oblique incidence, wave-covered surface. See text for further description.

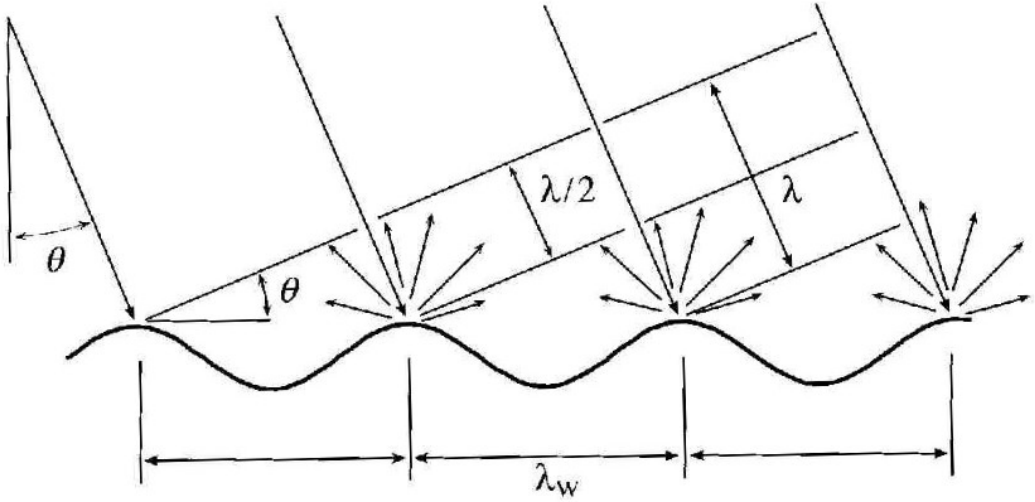

Figure 10.14. A schematic drawing of Bragg scatter modeled after the ERS-1 SAR. For the numbers given in the text, $\lambda_w = 72$ mm. See text for further description.

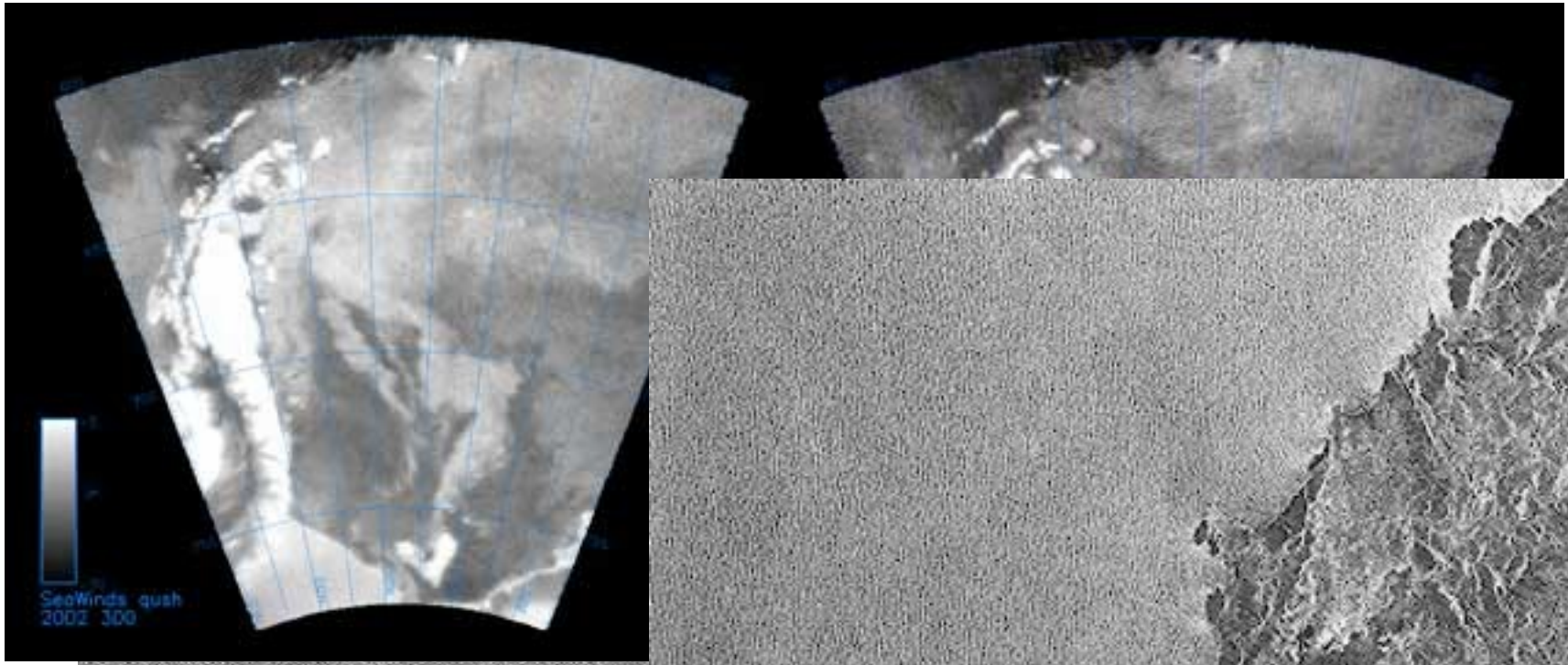

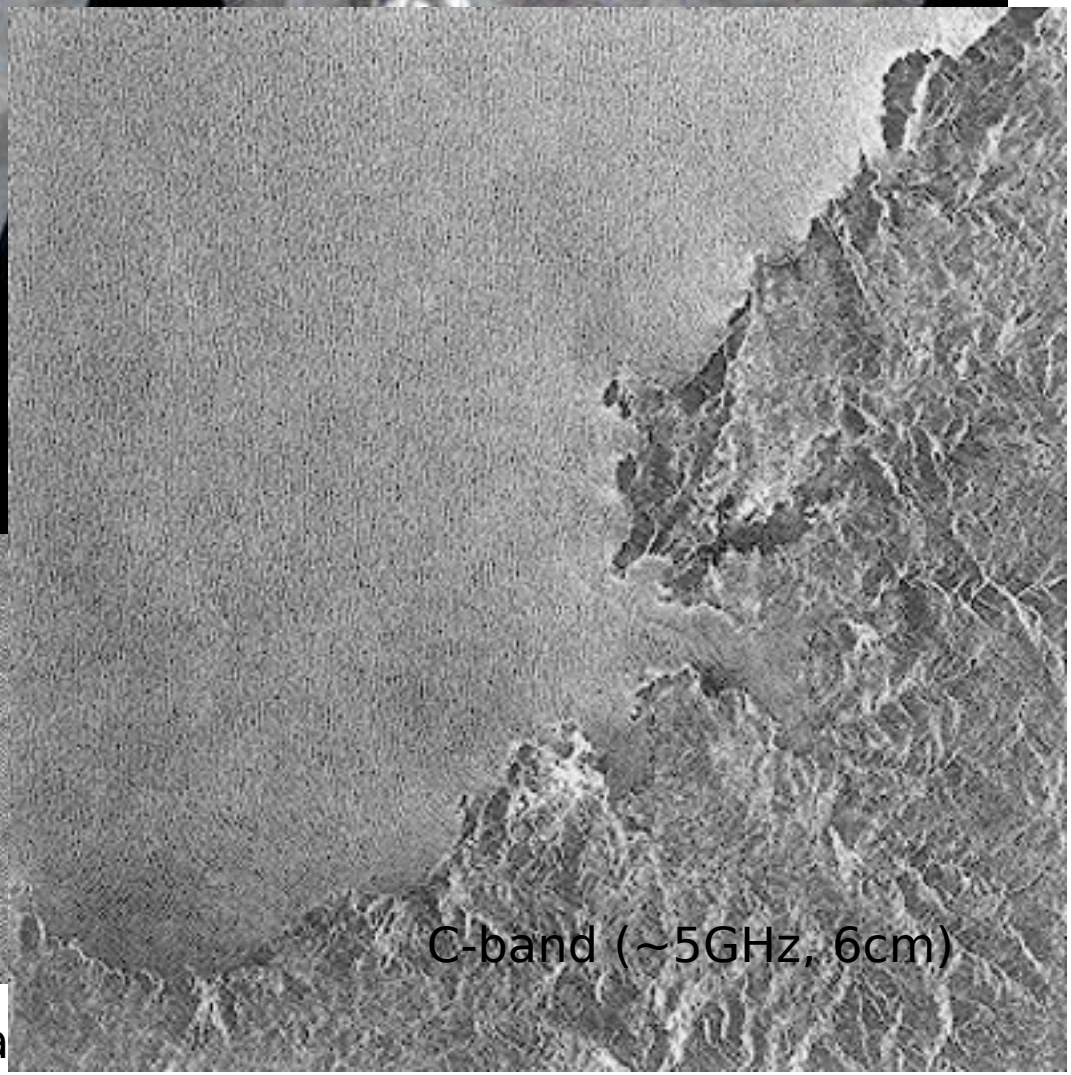

SeaSat image of North Sea L-ba
resolution 25m
SeaSat also had a Ku-band (~3cm)

Winds

- Winds are caused by air travelling from high pressure to low pressure regions
- On a large scale the rotation of the Earth is important

Boundary layers

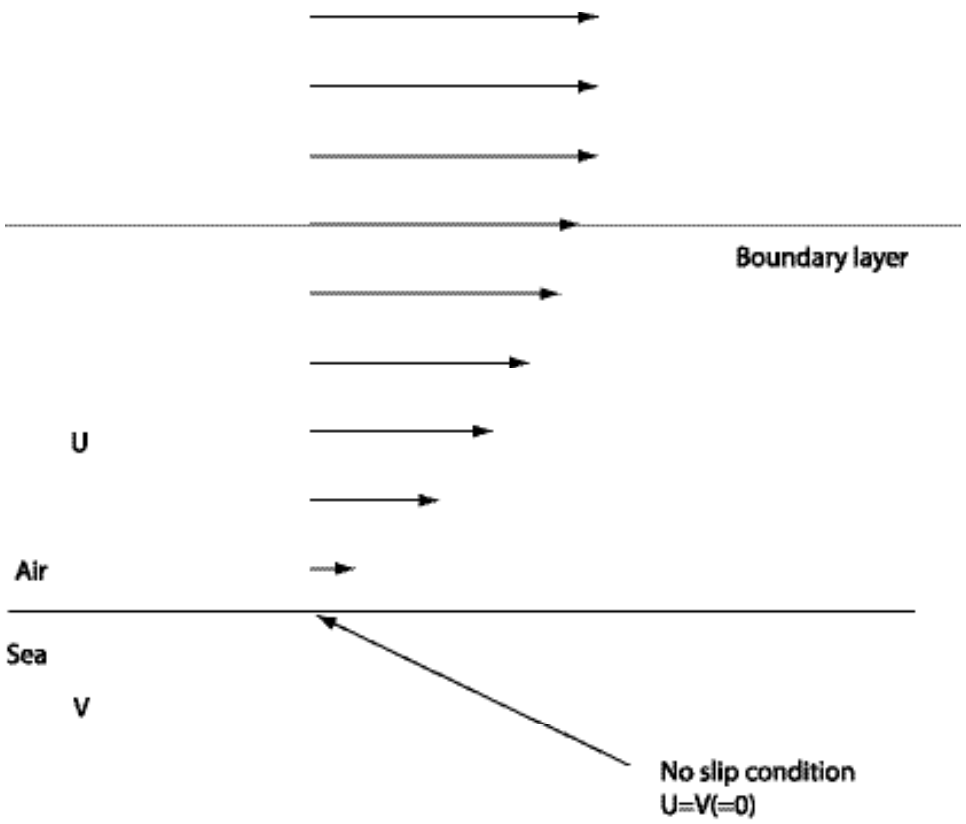

Stability

- The atmosphere is stable if the air temperature (T_{air}) is greater than the sea temperature (T_{sea})
- Unstable if $T_{air} < T_{sea}$
- Neutral if $T_{air} = T_{sea}$

Neutral stability winds

- In remote sensing we usually work with neutral stability winds
- Normally we work with winds at 10m height (U_{10})
- Sometimes people still quote winds at 19.5m ($U_{19.5}$)

Wind stress

- The wind *speed* at the surface almost zero
- The wind *stress* (u_*) is not.

$$U(z) = \frac{u_*}{\kappa} \ln\left(\frac{z}{z_0}\right)$$

κ is Von Karman's constant =0.4

z_0 is the roughness length

Waves

- Wind friction generates short waves
- Energy transfer to longer wavelengths
- Time evolving wave field
- Wave field also function of fetch

Gravity waves and capillary waves

- Gravity waves
  - “long” wavelengths ~ 0.1m upwards
  - Gravity is primary restoring force of oscillations
- Capillary waves
  - Wavelengths < 0.1 m
  - Oscillation affected also by surface tension

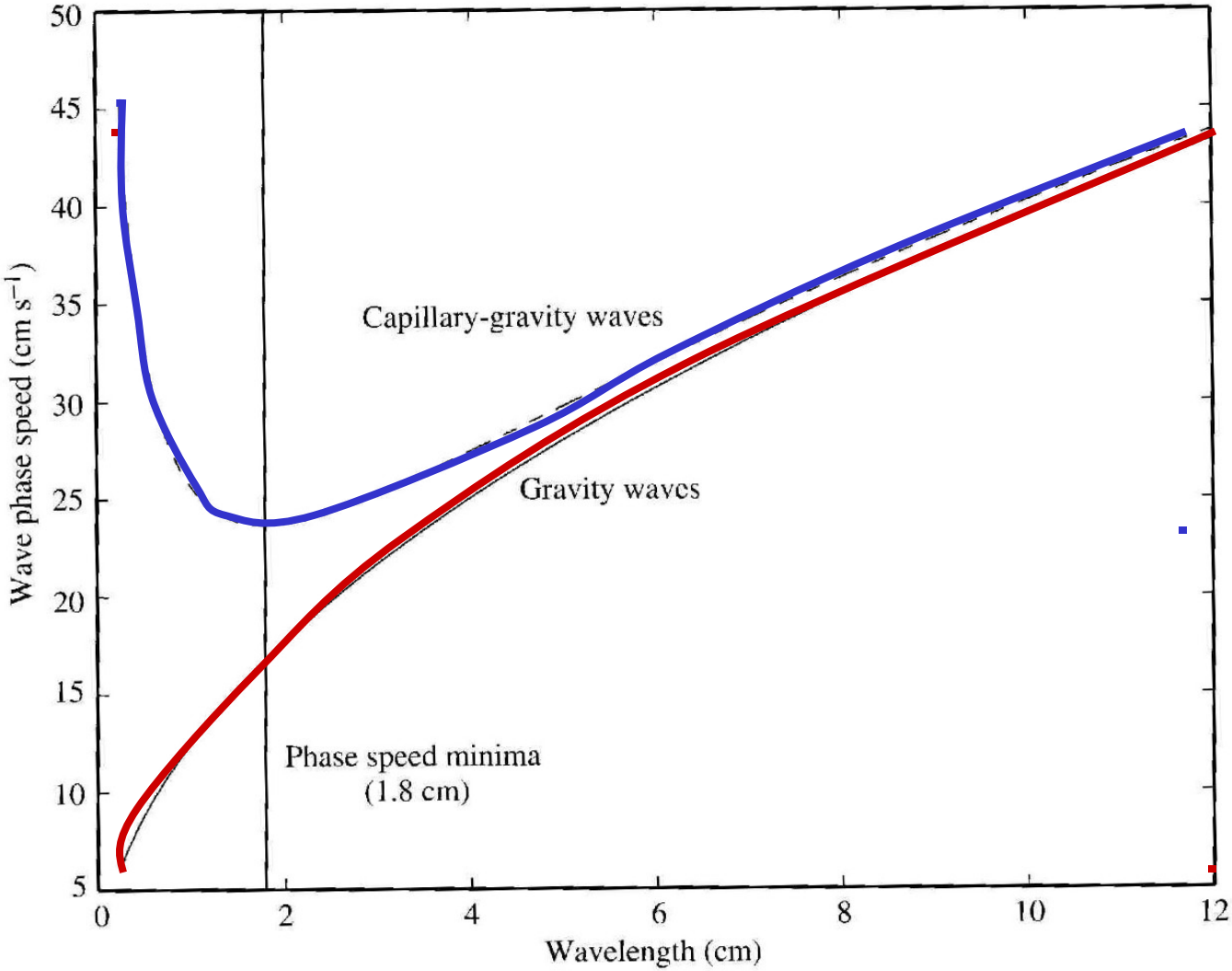

Figure 2.2. Comparison of the phase speed for capillary-gravity waves (dashed line) and for pure gravity waves (solid line) plotted versus wavelength for seawater. The vertical line marks the phase speed minimum for capillary waves. See text for additional information.

Sea and swell

- “Sea” identifies wave fields generated locally by the wind
  - Short waves, weakly non-linear (peaky crests, flat troughs)
- “Swell” identifies waves travelling in the area, having been generated elsewhere
  - longer waves, linear (regular sinusoid)

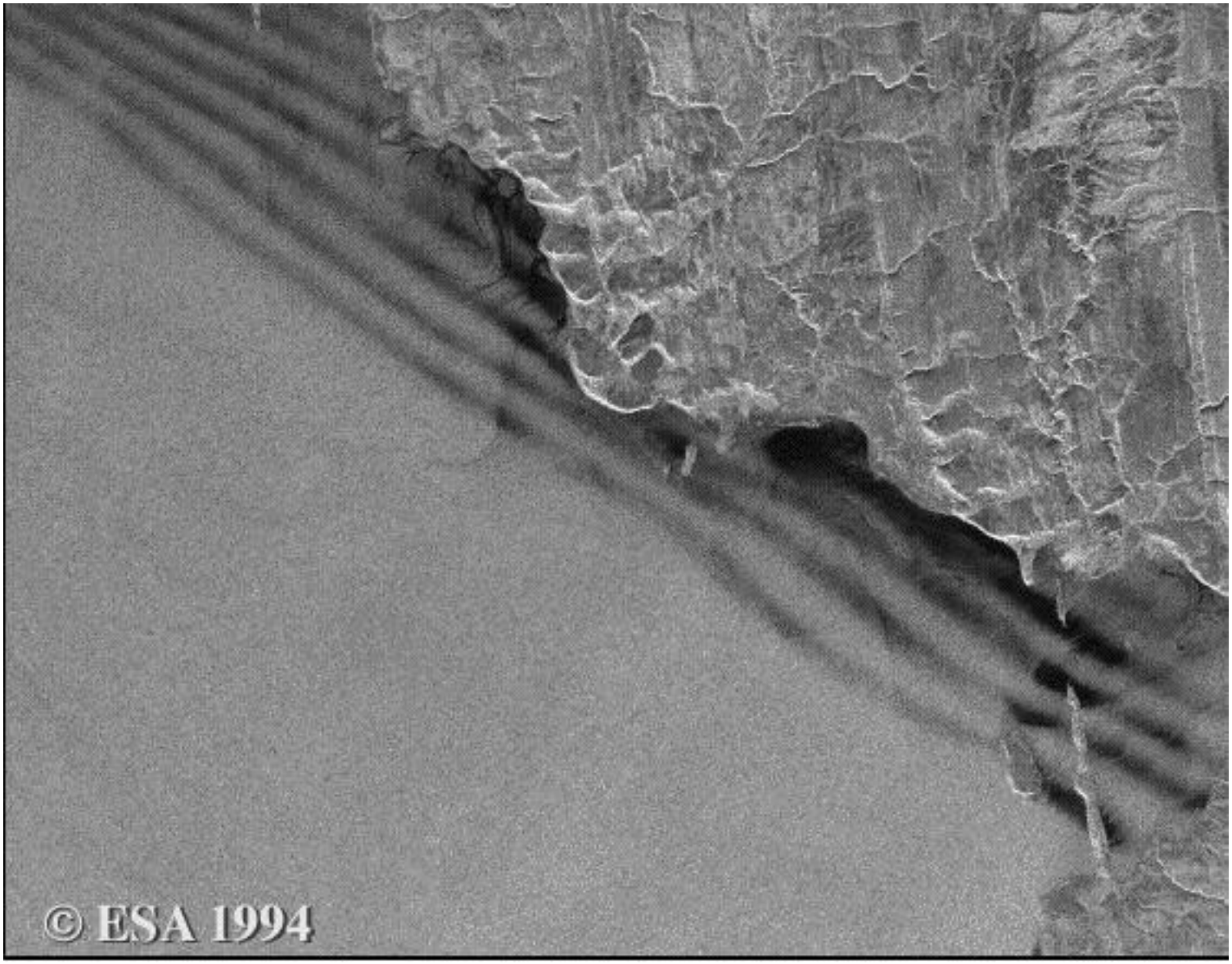

ERS-2 SAR image

A fully developed sea

- Theoretical concept
- Describes the state of the wave field when allowed to develop for an infinite duration and an infinite fetch, under a constant wind speed
- In reality, wind not constant over infinite duration/fetch

The wave spectrum

- Power spectral density of a record of elevation measurements
- Fourier transform of the record’s auto-correlation function
- Frequency spectrum S(w) and/or Wavenumber spectrum Sk(k)

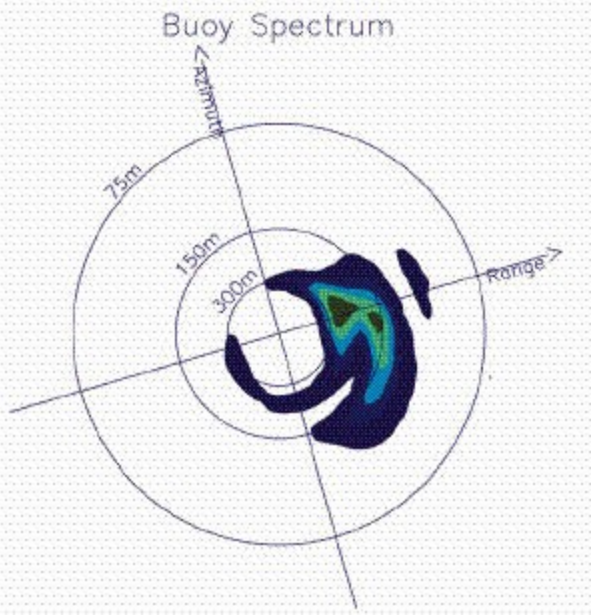

Significant wave height

- Average of the heights of the 1/3 highest waves
- Also known as H_s or $H_{1/3}$
- $H_{1/3} \sim 4\ \sigma_\xi$
- with σ_ξ = standard deviation of elevation record

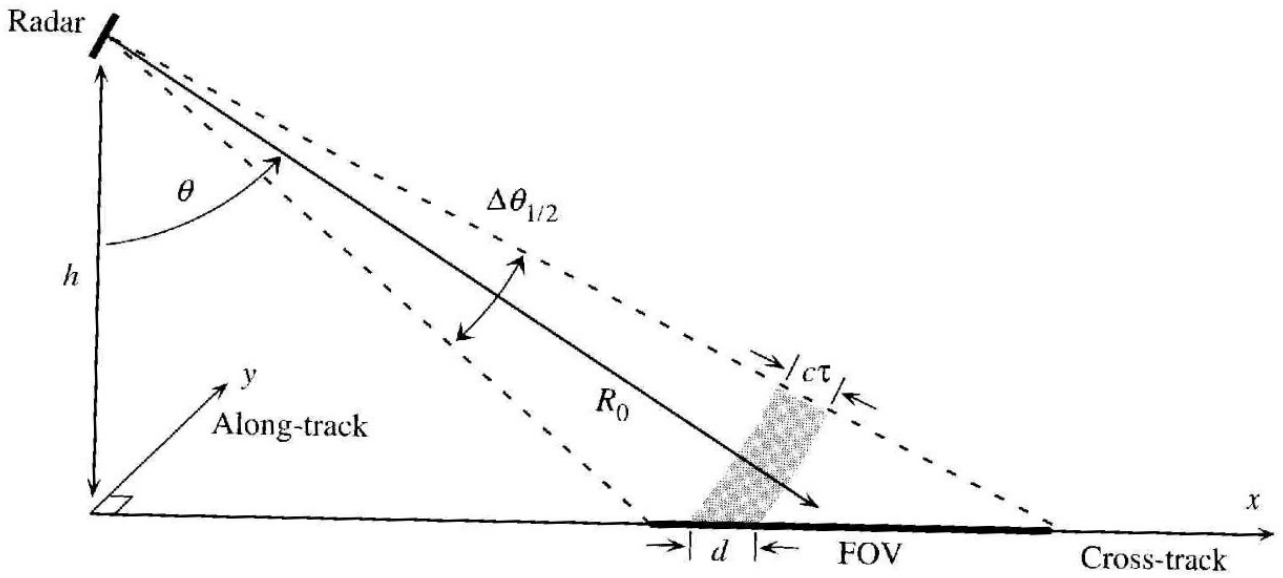

Figure 10.3. The interaction of a single pulse with the surface, where $c\tau$ is the pulse length and d is its projection on the surface.

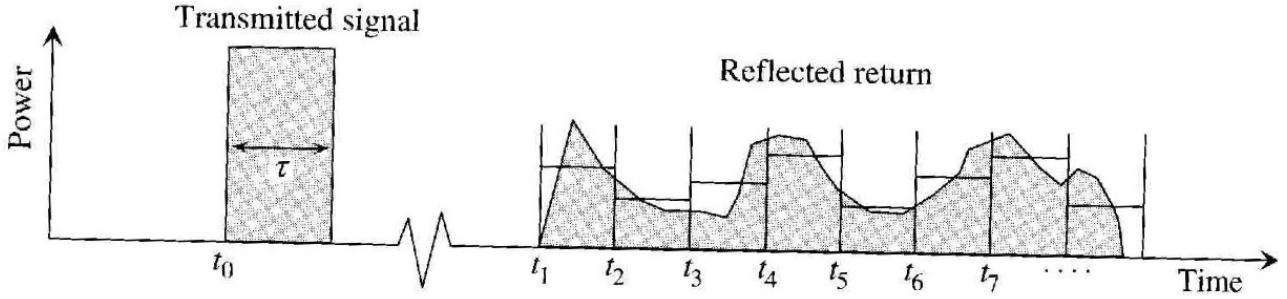

Figure 10.4. The binning of the radar return by time delay or range. The horizontal lines within each bin represent the average received power.

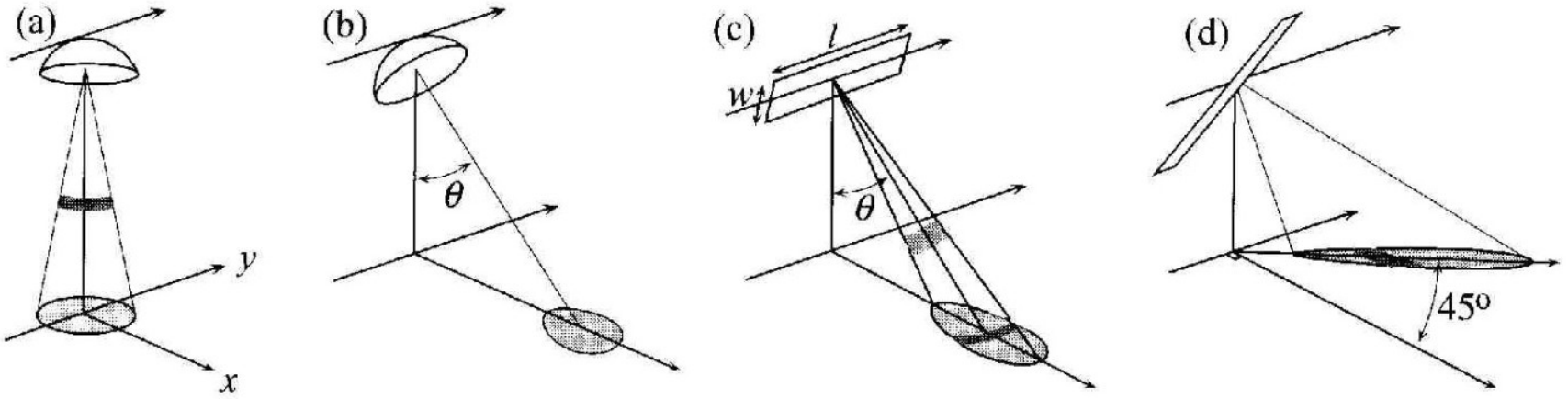

Figure 10.2. The configuration of four different antennas used in remote sensing. (a) The nadir-viewing altimeter parabolic antenna, (b) the side-looking parabolic antenna, (c) the side-looking rectangular antenna, (d) the scatterometer stick antenna, oriented at 45° to the flight path in a plane parallel to the surface. For each case, the light gray area on the surface is the FOV, while the dark gray swaths within the FOVs are in (c), a contour of constant range, and in (d), a contour of constant Doppler shift.

Active Microwave Instruments

Altimeters:

* Topex/Poseidon, 1992 - (Ku-band & C-band Topex; Ku-band Poseidon)
* Jason-1, Dec. 7, 2001 - (C-band & Ku-band)
* Geosat Follow On (GFO), U.S. Navy altimeter, February 1998 - (Ku-band)
* ICESat or GLAS (the Geoscience Laser Altimeter System), 2003 (LASAR - Visible ba

Scatterometers:

* SeaWinds, (on QuikScat, 1999 - present; on ADEOS-2, launched Dec. 13, 2002) (Ku-
* ERS-2 (European Remote Sensing Satellite 2) Scatterometer, 1995 - (C-band)

Synthetic Aperture Radars:

* Radarsat-1, 1995 -
* Envisat ASAR, March 2002 -(C-band)
* ERS-2 (European Remote Sensing Satellite 2) SAR, 1995 - (C-band)